J Appl Electrochem (2007) 37:483–489
DOI 10.1007/s10800-006-9279-8

ORIGINAL PAPER

Anomalous codeposition of Co–Ni: alloys from gluconate baths

M. M. Kamel

Received: 2 May 2006 / Accepted: 15 November 2006 / Published online: 13 January 2007

Abstract Thin films of cobalt–nickel alloys were galvanostatically deposited onto steel substrates from gluconate baths. Cathodic polarization curves were determined for the parent metals and Co–Ni alloy. The effects of bath composition, current density and temperature on cathodic current efficiency (CCE) and alloy composition were studied. The deposition of Co–Ni alloy is of anomalous type, in which the less noble metal (Co) is preferentially deposited. The CCE of codeposition is high and increases with increase in temperature and current density, but it decreases as the $[Co^{2+}]/[Ni^{2+}]$ ratio in the bath increases. The percentage of Co in the deposit increases with increasing cathodic current density, temperature and increasing Co^{2+} ion concentration. The structure and surface morphology of the deposit were studied by XRD, ALSV and SEM. The results showed that the alloys consisted of a single solid solution phase with a hexagonal close packed structure.

Keywords Anomalous codeposition · Co–Ni alloys · Gluconate baths

1 Introduction

Amorphous ferromagnetic films are widely used in the microelectronics industry, magnetic media and computers [1]. Different methods are used in the preparation of these films. Electrodeposition is a good technique for preparing highly functional magnetic recording materials. It offers the advantage of low-cost production, since it requires simple and inexpensive processing equipment. Moreover, electrodeposition technique is suitable for producing multi-layers with a large area and arbitrary shape [2, 3].

Nickel, cobalt and their alloys are important engineering materials. They have unique properties, such as magnetic, wear-resistant, heat-conductive, light-reflector and electrocatalytic activity [4–6]. In addition, Ni and Co oxides are used in batteries [7, 8]. The physico-chemical properties of alloys are seriously affected by their composition and structure [9–12]. Therefore, reliable control of their composition and structure is an important issue for their wide application [13].

Cobalt and nickel forms a solid solution over the whole concentration range [14]. This ability enables the potential uses of their magnetic properties in a wider range of conditions. This makes Co–Ni alloy of special interest to the microelectronics industry [15, 16]. Further, Co–Ni films are expected to show greater resistance to corrosion than Ni–Fe films [1].

The electrodeposition of Co–Ni alloys, whether from simple or complex baths, is a codeposition of anomalous type [1, 16–21]. The less noble metal, Co, deposits preferably to the nobler one, Ni. The operating conditions such as current density, temperature, pH, use of organic additives, buffer capacity, concentration of all solution components, etc. lead to changes in the kinetics of electrodeposition, the composition and morphology of the coatings and their physico-mechanical characteristics.

The majority of metal electrodeposition processes are carried out from baths containing complexing

M. M. Kamel (✉)
Chemistry Department, Faculty of Science, Suez Canal University, Ismailia 41522, Egypt
e-mail: madhet_kamel@yahoo.com

agents. Recently, the various complexing agents such as sulfamates, tartrates, citrates, glycinates and gluconates have been used. These complexing agents are non-toxic, easily obtained and their degradation products offer easier treatment [22].

The purpose of the present investigation is to obtain cobalt–nickel electroplates with good quality from acidic gluconate baths. Such baths are not only cheap but also environmentally friendly. The effect of bath composition and some operating parameters on cathodic polarization and cathodic current efficiency (CCE) was investigated. The composition and structure of the deposits were also examined.

2 Experimental details

Co–Ni alloys were obtained from baths of composition: 0.02–0.12 M $CoSO_4 \cdot 7H_2O$, 0.08–0.18 M $NiSO_4 \cdot 6H_2O$, 0.20 M anhydrous Na_2SO_4 and 0.20–0.50 M $C_6H_{11}O_7Na$. The total concentration of metal sulphates was kept constant (0.20 M) in the plating bath. All solutions were freshly prepared with distilled water and analytical grade chemicals. The pH was adjusted at 5 using sulphuric acid or sodium hydroxide and measured via Fisher Scientific pH-meter.

The experimental setup for the electrodeposition process consisted of a rectangular Perspex cell containing 70 cm^3 of electrolyte solution. The cathode was a 3×3 cm^2 steel plate and the anodes were stainless steel with total exposed area of 18 cm^2. The anodes were held in contact with the walls of the cell and the cathode was positioned midway between them. The cathode was mechanically polished with progressively finer grades of emery paper, washed with distilled water, rinsed with ethanol and weighed. The deposition was carried out from stagnant solutions. Experiments were conducted at the required temperatures with the help of an air thermostat ± 1 °C. The plating time was 20 min, after which the cathode was withdrawn, washed with distilled water, ethanol, dried and weighed. The alloy composition was determined by atomic absorption spectrophotometer Perkin–Elmer model 2380, after dissolving the deposited alloy in a mixture of concentrated hydrochloric and nitric acids and diluting the solution with distilled water to 100 ml.

For each electrodeposition condition at least three separate tests were carried out. The percentage of cobalt in baths and deposits was calculated according to the following relation [23]:

$$\%\,\text{of Co} = \frac{mass\ of\ Co}{mass\ of\ Co\ +\ mass\ of\ Ni} \times 100$$

The galvanostatic cathodic polarization measurements were conducted in a three-electrode cell provided with a steel cathode of area 0.785 cm^2. A stainless steel wire was used as an anode and saturated calomel (SCE) as a reference electrode. The potential of the working electrode was measured by a potentiometer (Sargant Welch Scientific Co, Skokie, IL, USA). The current was applied in 2 mA increments and the corresponding potential was measured after 1 min.

The stripping voltammetry measurements were made in the three-electrode cell, where the working electrode was a glassy carbon disk of area 1 cm^2. The counter electrode was a platinum wire and the reference electrode was SCE. The electrodes were connected to a potentiostat/galvanostat, model 273 controlled by a microcomputer. The alloys were deposited onto glassy carbon electrodes at a particular potential (deposition potential) for 100 s. Each deposition was followed directly by scan stripping voltammetry with scan rate 10 mV s^{-1} without removing the electrode from the plating solution.

The phase and crystal structure of the deposited alloy were investigated using Siemens D 500 X-ray diffractometer at 35 KV and 15 mA. The surface morphology was examined using Joel model JSM -T-100 scanning electron microscopy.

3 Results and discussion

3.1 Galvanostatic cathodic polarization

Figure 1 shows the galvanostatic cathodic polarization curves for the deposition of cobalt (curve a), nickel (curve b) and Co–Ni alloy (curve c) under identical conditions. The deposition does not occur until the cathodic potential attains –1.3 V for Co, –1.55 V for Ni and –1.50 V for Co–Ni alloy. This result indicates that extra energy (more negative potential) is needed to overcome the barrier of heterogeneous deposition onto a foreign substrate [24]. In addition, the deposition from electrolyte solutions containing complexing ions is accompanied by large polarization. Nickel exists as $[Ni\ C_6H_{11}O_7]^+$ complex ($K_f = 74.43$) [25]. Cobalt is present as unstable cationic species $[Co\ C_6H_{11}O_7]^+$ ($K_f = 1.45 \times 10^{-8}$) [26]. The cathodic polarization curve of cobalt exhibits a limiting current plateau. This

implies that under the limiting conditions, the deposition of cobalt is controlled by diffusion of Co^{2+} ions.

The experimental polarization curve of Co lies at more noble potentials than that of Ni. This indicates that Co is the nobler metal in the present system. The polarization curve of the alloy lies between those of the parent metals. The codeposition enables the less noble metal to codeposit at less cathodic potentials and the more noble metal to deposit at more cathodic potentials than in the individual deposition cases [27]. The given data suggest that in alloy deposition, cobalt would be deposited much more readily than nickel. Therefore, the deposition of Co–Ni alloy from gluconate baths is of anomalous type [23].

The partial current densities of each metal (i_p) during codeposition could be calculated from deposit composition (w), the deposition time (t), the mass of the deposit (m) and the electrochemical equivalent (e) [28].

$$i_p = \frac{m\,w}{100\,e\,t}$$

The hydrogen partial current density was determined by subtracting the sum of the metal current densities from the total applied current density. Dashed curves in Fig. 1, represent the partial current densities for Co, Ni and H_2 during codeposition. The deposition rate of Ni is lower than that of Co but higher than the rate of hydrogen evolution. The data of Table 1 show that the partial current densities of nickel and hydrogen are small. This implies the production of alloy with low-nickel content and high-current efficiency.

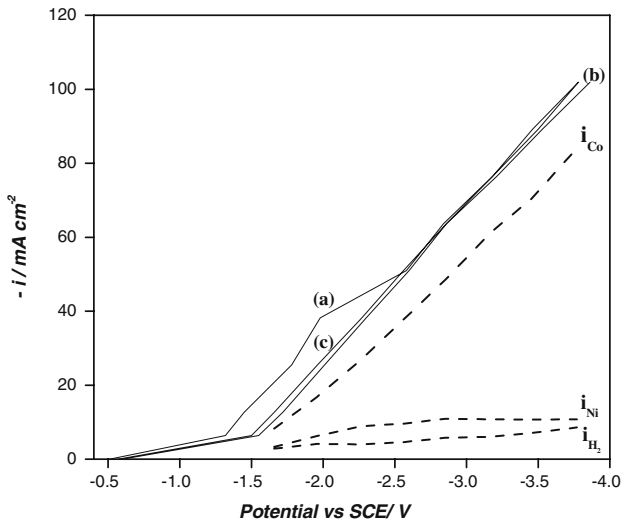

Fig. 1 Galvanostatic cathodic polarization curves obtained at pH 5 and 25 °C for the electrodeposition of (a) cobalt from solution containing 0.04 M $CoSO_4 \cdot 7H_2O$; (b) nickel from solution containing 0.16 M $NiSO_4 \cdot 6H_2O$; (c) Ni–Co alloy from solution containing 0.04 M $CoSO_4 \cdot 7H_2O$ and 0.16 M $NiSO_4 \cdot 6H_2O$. Each solution contained 0.20 M Na_2SO_4 and 0.30 M $C_6H_{11}O_7Na$ (- - - -) calculated curves for Co, Ni and H_2

The electrodeposition of Co–Ni alloy is of anomalous type in which the less noble metal (Co) is preferentially deposited. This expressed by the much higher percentage of Co in the deposit than in the bath. The anomalous codeposition of Co–Ni alloy was explained by near electrode pH change and competitive adsorption, underpotential deposition and fast kinetics of reduction of high-spin Co(II) complexes [29–32]. Increasing the pH at the cathode interface is generally responsible for the inhibition of nickel discharge in the hydroxide suppression mechanism [33]. The present work does not seem to confirm this theory, since the partial current density of hydrogen remains quite constant and very low, Fig. 1. Also, the anomalous codeposition of Co–Ni alloy could not be assigned to the underpotential deposition of cobalt as the deposition potential of the latter (–1.3 V versus SCE) is more negative than the equilibrium value (–0.52 V versus SCE). Therefore, the inhibition of nickel ion reduction could be attributed to the intrinsically slow nickel kinetics. The same result was obtained by Mathias and Chapman for zinc–nickel alloys [34, 35].

Figure 2 shows that the cathodic polarization of alloy deposition shifts slightly to more negative values as the concentration of sodium gluconate increases from 0.20 to 0.50 M. This is mainly attributed to increasing stability of Ni^{2+}– gluconate complex species.

3.2 Composition of Co–Ni electrodeposited alloy

Figures 3–6 show the CCE of Co–Ni alloy and the percentage of cobalt in the deposit as a function of some plating variables. Composition Reference Line (CRL) represents the percentage of Co in the bath. The CCE is less than 100% as a result of simultaneous discharge of hydrogen ions. The percentage of Co in the deposit is larger than its percentage in the bath, indicating that the deposition of Co–Ni alloy is of anomalous type [23].

Figure 3 shows the influence of $[Co^{2+}]/[Ni^{2+}]$ ratio in the bath on the percentage of Co in the deposit and on the CCE of alloy deposition. The Co percentage in the deposit increases from 72 to 92% as the $[Co^{2+}]/[Ni^{2+}]$ ratio increases from 0.11 to 1.50. This is due to an increase in the efficiency of Co deposition at the expense of Ni. An increase in Co^{2+} concentration tends to oppose the depletion of Co^{2+} ions in the cathodic diffusion layer [36]. Increasing the $[Co^{2+}]/[Ni^{2+}]$ ratio

Table 1 Partial current densities for Co, Ni and H_2 during the electrodeposition of Co–Ni alloy from a bath containing 0.04 M $CoSO_4 \cdot 7H_2O$, 0.16 M $NiSO_4 \cdot 6H_2O$, 0.20 M Na_2SO_4 and 0.30 M $C_6H_{11}O_7Na$ at pH 5 and 25 °C

Current density /mA cm^{-2}	–Potential /V	Partial current densities/mA cm^{-2}		
		i_{Co}	i_{Ni}	i_{H2}
12.74	1.66	7.70	2.74	2.30
25.48	1.96	16.25	5.68	3.55
38.22	2.27	26.44	8.36	3.42
63.69	2.86	48.10	10.36	5.23
101.91	3.78	83.73	10.19	7.99

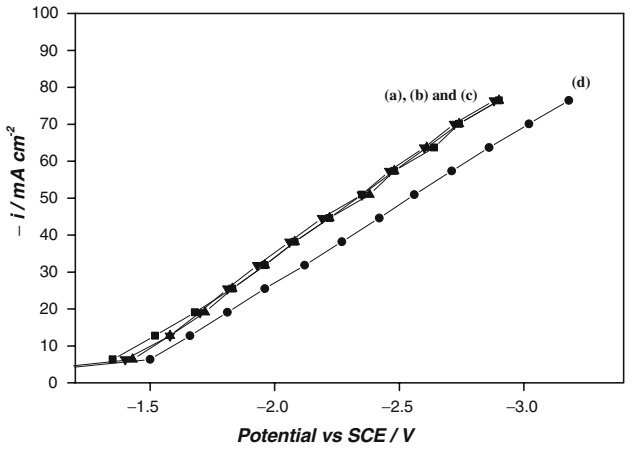

Fig. 2 Galvanostatic cathodic polarization curves for the deposition of Ni–Co alloy on steel at pH 5 and 25 °C from solutions containing 0.04 M $CoSO_4 \cdot 7H_2O$, 0.16 M $NiSO_4 \cdot 6H_2O$ and 0.20 M Na_2SO_4 and different concentrations of $C_6H_{11}O_7Na$: (a) 0.20, (b) 0.30, (c) 0.40 and (d) 0.50 M

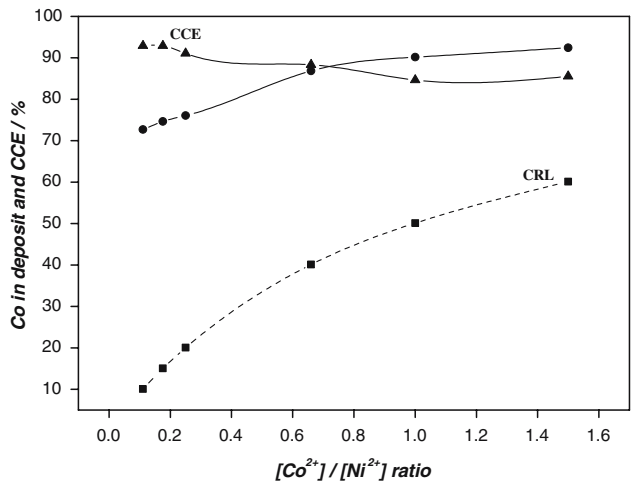

Fig. 3 Effect of $[Co^{2+}]/[Ni^{2+}]$ ratio on CCE and percentage of Co in the deposits from bath containing 0.20 M Na_2SO_4 and 0.30 M $C_6H_{11}O_7Na$ at cd = 5.02 mA cm^{-2}, pH 5, t = 20 min and 25 °C. *CRL* represents the percentage of Co in the bath

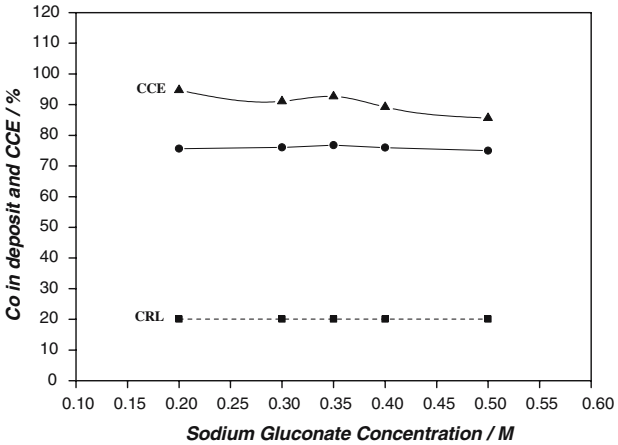

Fig. 4 Effect of $C_6H_{11}O_7Na$ concentration on CCE and percentage of Co in the deposits from bath containing 0.04 M $CoSO_4 \cdot 7H_2O$, 0.16 M $NiSO_4 \cdot 6H_2O$ and 0.20 M Na_2SO_4 at cd = 5.02 mA cm^{-2}, pH 5, t = 20 min and 25 °C. *CRL* represents the percentage of Co in the bath

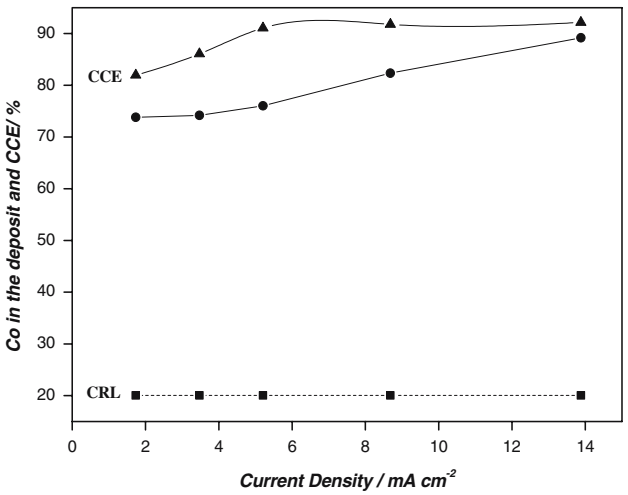

Fig. 5 Effect of current density on CCE and percentage of Co in the deposits from bath containing 0.04 M $CoSO_4 \cdot 7H_2O$, 0.16 M $NiSO_4 \cdot 6H_2O$, 0.20 M Na_2SO_4 and 0.30 M $C_6H_{11}O_7Na$ at pH 5, t = 20 min and 25 °C. *CRL* represents the percentage of Co in the bath

leads to a decrease in the CCE due to a large decrease in the efficiency of Ni deposition.

Figure 4 shows that an increase in the sodium gluconate concentration tends to decrease the CCE for Co–Ni deposition but it has no effect on the composition of the deposit. This is due to an increase in the stability of Ni^{2+}– gluconate complex species and consequent inhibition of the reduction of nickel at the expense of the reduction of hydrogen.

Figure 5 illustrates the effect of current density on alloy composition and CCE for alloy deposition. The

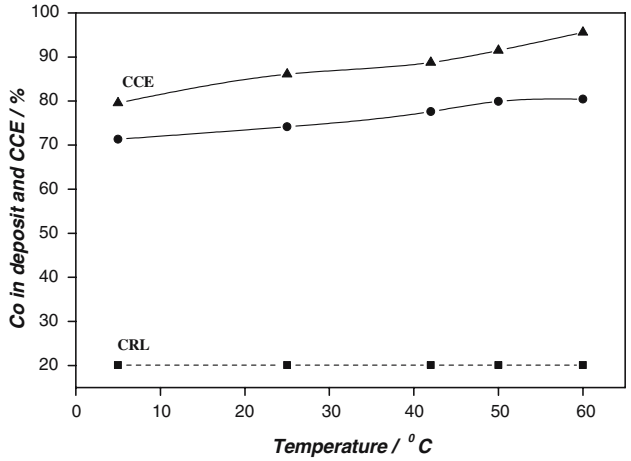

Fig. 6 Effect of temperature on CCE and percentage of Co in the deposits from bath containing 0.04 M $CoSO_4 \cdot 7H_2O$, 0.16 M $NiSO_4 \cdot 6H_2O$, 0.20 M Na_2SO_4 and 0.30 M $C_6H_{11}O_7Na$ at cd = 3.47 mA cm^{-2}, pH 5 and t = 20 min. *CRL* represents the percentage of Co in the bath

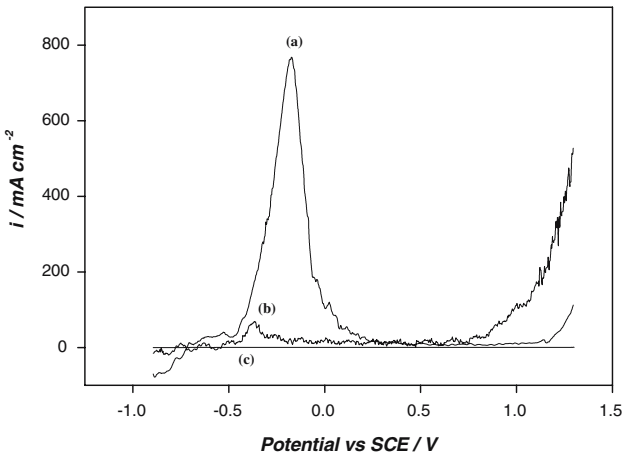

Fig. 7 Linear sweep voltammogram of a fixed glassy carbon electrode in various solutions: (a) 0.04 M $CoSO_4 \cdot 7H_2O$ (deposition potential –1.3 V versus SCE); (b) 0.16 M $NiSO_4 \cdot 6H_2O$ (deposition potential –1.5 V versus SCE); (c) 0.04 M $CoSO_4 \cdot 7H_2O$ and 0.16 M $NiSO_4 \cdot 6H_2O$ (deposition potential –1.5 V versus SCE). Each solution containing 0.2 M Na_2SO_4 and 0.3 M $C_6H_{11}O_7Na$. The deposition time = 100 s. Sweep rate = 10 mV s^{-1}

CCE increases with current density as a result of increasing the cathodic polarization. This assists the discharge of cobalt ions. Therefore, the cobalt content in the deposit increases with current density.

The effect of temperature on Co content in the deposit and on the CCE of alloy deposition is illustrated in Fig. 6. The Co content in the deposit and the CCE increases slightly with temperature. The influence of temperature on the composition of an alloy deposited in anomalous codeposition is determined by two opposing factors: polarization and diffusion. On increasing the temperature, the first factor, polarization, tends to increase the content of the more noble metal in the deposit. However, the second factor, diffusion, favours the deposition of the less noble metal. It seems that the influence of diffusion predominates over that of polarization and the cobalt content of the deposits increases with temperature. The CCE of alloy deposition increases with temperature due to an increase in the efficiency of codeposition [22, 37].

3.3 Anodic dissolution of Co–Ni alloy coatings

To analyze the obtained deposits in situ, potentiodynamic stripping (ALSV) was performed. This technique is very useful in characterizing the electrodeposited alloy [38]. For this purpose, the electrodeposits were obtained potentiostatically under stationary conditions for 100 s and immediately oxidized by means of voltammetric scan at 10 mV s^{-1}. Figure 7 illustrates the anodic curves for the dissolution of Co, Ni and Co–Ni coatings. For the dissolution of Co coating, curve a, a dissolution peak appears at a potential –182 mV versus SCE. Ni coating exhibits a dissolution peak at a potential –376 mV versus SCE, curve b. This result indicates that cobalt coating is more corrosion resistant than nickel coating. During the dissolution of Ni coating, a current oscillation was observed which could be attributed to the intensive hydrogen evolution over nickel coating [39]. The voltammogram of the Co–Ni alloy does not exhibit any dissolution peaks. This result indicates that Co–Ni alloy is completely passive in the plating bath and sodium gluconate is a good inhibitor. Rashwan obtained the same result for Co–Ni alloy in citrate bath [40]. Refaey [41] reported that the anodic dissolution is inhibited by adsorption of gluconate ions on the metal surface or on the oxide passive film.

3.4 Structure characterization

Most of the obtained deposits were compact and fine-grained. Because of the high density of nuclei, coalescence occurred at low-deposition times, so that individual grains could not be resolved. The metallic lustre and brightness of the deposit increase with increasing Ni^{2+} ion concentration. Increasing the current density improves the brightness of the deposits. However, increasing the bath temperature leads to the formation of dark grey deposits.

The surface morphology of the as—deposited Co–Ni alloys obtained under different plating conditions were

examined by SEM. Some of the SEM micrographs are shown in Fig. 8. The deposit obtained at low-current density (Co_{74}–Ni_{26}) is smooth and compact. It consists of regularly oriented columnar grains, Fig. 8a. This result indicates a low-nucleation rate but high-growth rate for low overpotentials [42]. At high-current density, the deposit (Co_{89}–Ni_{11}) is not uniform and composed of irregular grains. These grains are grouped together in random orientations and include some pores. These features appear to be related to evolved and/or absorbed hydrogen on the cathode surface, Fig. 8b.

XRD data show that Co–Ni form solid solutions and this enables the alloys to be obtained with different proportions of the two metals. This is in agreement with previously published data on the deposits obtained from chloride and acetate electrolytes [43, 44].

Figure 9 shows XRD patterns for Co–Ni coatings obtained at different current densities. Next to the peaks corresponding to the steel substrate, five well-defined peaks are observed. The peaks are sharp and well defined, indicating good crystallization structure. All indexed peaks correspond to a hexagonal close packed structure [16, 40]. At low-current density, the alloy exhibits a (002) growth orientation with significant (100), (101), (110) and (004) reflections as well. The diffractograms indicate that the alloy deposits have a preferred orientation of (002).

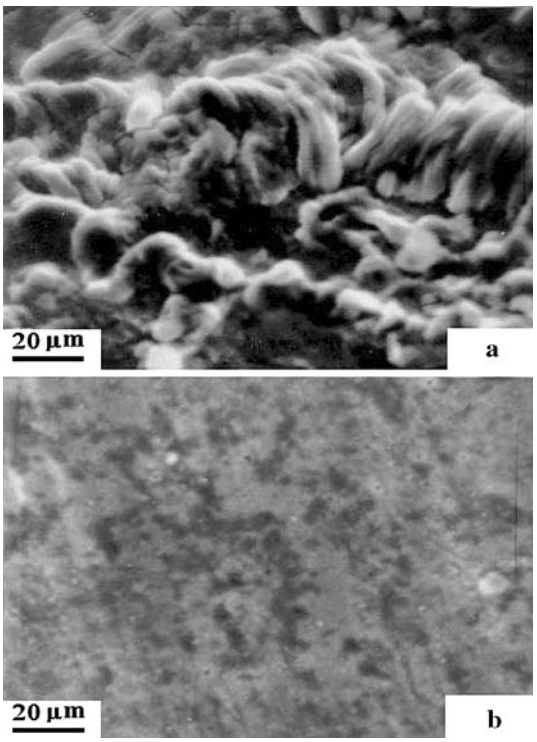

Fig. 8 SEM micrograghs of the Co–Ni electrodeposits obtained from a bath containing 0.04 M $CoSO_4 \cdot 7H_2O$, 0.16 M $NiSO_4 \cdot 6H_2O$, 0.20 M Na_2SO_4 and 0.30 M $C_6H_{11}O_7Na$ at pH 5 and t = 20 min, 25 °C and at different current densities: (a) 3.47 and (b) 13.88 mA cm^{-2}

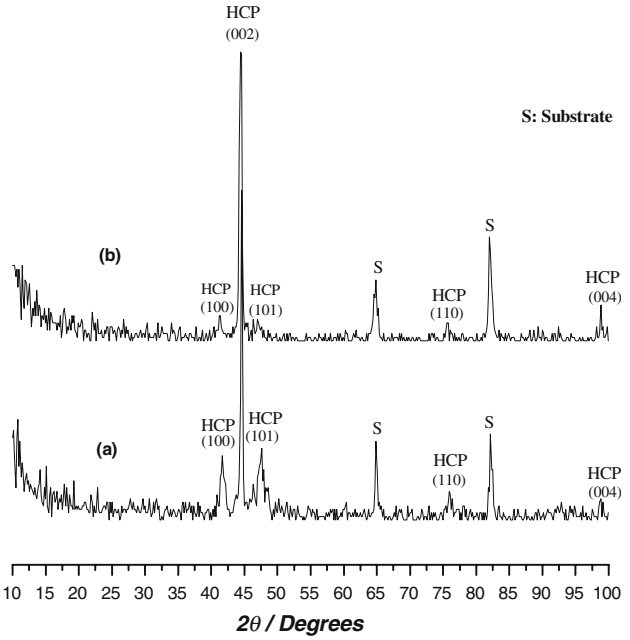

Fig. 9 X-ray diffraction patterns of electrodeposited Co–Ni alloy obtained from a bath containing 0.04 M $CoSO_4 \cdot 7H_2O$, 0.16 M $NiSO_4 \cdot 6H_2O$, 0.20 M Na_2SO_4 and 0.30 M $C_6H_{11}O_7Na$ at pH 5 and t = 20 min, 25 °C and at different current densities: (a) 3.47 and (b) 13.88 mA cm^{-2}

Increasing the applied current density to 13.88 mA cm^{-2} decreases the intensity of the planes (100), (101) and (110). The observation of a single diffraction angle for the planes (002) can be interpreted such that cobalt and nickel share the same lattice parameter. Also, the interfaces between cobalt and nickel are coherent [36, 45].

4 Conclusion

Smooth, compact and bright deposits of Co–Ni alloy can be electrodeposited onto steel substrates from gluconate baths. The deposition of Co–Ni alloy is of anomalous type. The intrinsically slow kinetics of nickel is mainly responsible for the anomalous codeposition. The cathodic efficiency is high and depends on the applied current density and temperature. The composition of the deposit is strongly affected by the applied current density and $[Co^{2+}]/[Ni^{2+}]$ ratio in the bath. ALSV measurements show that the Co–Ni coating is completely passive in gluconate baths. The deposited alloys consist of a single solid solution phase with a hexagonal-close packed structure.

References

1. Gomez E, Ramirez J, Valles E (1998) J Appl Electrochem 28:71
2. Lopez Anton R, Fdez Gubieda ML, Garcia Arribas A, Herreros J, Insausti M (2002) Mater Sci Eng A335:94
3. Gomez E, Labarta A, Liorente A, Valles E (2002) Surf Coating Technol 153:261
4. Hu CC, Weng CY (2000) J Appl Electrochem 30:499
5. Hu CC, Bai A (2001) J Appl Electrochem 31:565
6. Jones RM, Iulia MC, Zimmerman RD (2002) Proc SPIE Int Soc Opt Eng 4849:77
7. Maurel F, Knosp B, Backhaus Ricoult M (2000) J Electrochem Soc 147:78
8. Wang CC, Goto KS, Akbar SA (1991) J Electrochem Soc 138:3673
9. Schwarzacher W, Lashmore DS (1996) IEEF Trans Hagn MAG 32:3133
10. Osaka T (1999) Electrochim Acta 44:3855
11. Osaka T, Takai M, Ohashi K, Saito M, Yamada K (1998) Nature 392:796
12. Yin KM (1997) J Electrochem Soc 144:1560
13. Bai A, Hu CC (2002) Electrochim Acta 47:3447
14. Barker H (ed.) (1992) ASM handbook. ASM International, Ohio
15. Gomez E, Valles E (1999) J Appl Electrochem 29:805
16. Golodnitsky D, Rosenberg Y, Ulus A (2002) Electrochim Acta 47:2707
17. Abdel-Rehim SS, Abd El-Halim AM, Osman MM (1985) J Appl Electrochem 15:107
18. Abd El-Halim AM (1986) Surf Coatings Technol 27(2):103
19. Fan C, Piron DL (1996) Electrochim Acta 41:1713
20. Chi BLJ, Yang XGY, Gong YWN (2005) Int J Hydrogen Energy 30(1):29
21. Correia AN, Machado SAS (2000) Electrochim Acta 45:1713
22. Rashwan SM, Mohamed AE, Abd El-Wahaab SM, Kamel MM (2003) J Appl Electrochem 33:1035
23. Brenner A (1963) Electrodeposition of alloys, vol 1. Academic Press, New York
24. Lin YP, Selman JR (1993) J Electrochem Soc 140(5):1299
25. Kouba A (1975) Surfaces 93:81
26. Ashton JF, Pickering WF (1970) Aust J Chem 23(7):1367
27. Abd El-Rehim SS, Refaey SA, Gebel GS, Taha F, Saleh MB (1995) J Appl Electrochem 25:1
28. Sridharan K, Sheppard K (1997) J Appl Electrochem 27:1198
29. Golodnitsky D, Gudin NV, Volyanuk GA (2000) J Electrochem Soc 147(11):4156
30. Zech N, Podlaha EJ, Landolt D (1999) J Electrochem Soc 146(8):2886
31. Gadad S, Harris TM (1998) J Electrochem Soc 145(11):3699
32. Goldbach S, de Kermadec R, Lapicque F (2000) J Appl Electrochem 30:277
33. Fratesi R, Roventi G, Giuliani G, Tomachuk CR (1997) J Appl Electrochem 27:1088
34. Mathias MF, Chapman TW (1987) J Electrochem Soc 134:1408
35. Mathias MF, Chapman TW (1990) J Electrochem Soc 137:102
36. Mohamed AE, Rashwan SM, Abd El-Wahaab SM, Kamel MM (2003) J Appl Electrochem 33:1085
37. Albalat R, Gomez E, Muller C, Pergonas J, Sarret M, Valles E (1991) J Appl Electrochem 21:44
38. Despic AR, Jovic VD (1995) Modern aspects of electrochemistry. Plenum, New York
39. Lin YP, Robert Selman J (1993) J Electrochem Soc 140(5):1299
40. Rashwan SM (1999) Metall 53(12):686
41. Refaey SAM (1996) J Appl Electrochem 26:503
42. Rashwan SM, Mohamed AE, Abd El-Wahaab SM, Kamel MM (2000) Mans Sci Bull 27(1):121
43. Singh VB, Singh VN (1976) Plat Surf Finish 7:34
44. Myung NV, Nobe K (2001) J Electrochem Soc 148(3):136
45. Bradely PE, Landolt D (1999) Electrochim Acta 45:1077